

Impact of Absorbing Layer Band Gap and Light Illumination on the Device Performance of a Single Halide Cs₂TiX₆ Based PSC

K. Chakraborty¹, S. Paul^{1*}, U. Mukherjee², S. Das³

¹ *Advanced Materials Research and Energy Application Laboratory, Department of Energy Engineering, North-Eastern Hill University, Shillong 793022 Meghalaya, India*

² *Department of Life Science, VIT College, Midnapore-721101 West Bengal, India*

³ *Department of Electronics and Communication Engineering, IMPS College of Engg. and Tech., Malda 732103, West Bengal, India*

(Received 10 January 2021; revised manuscript received 15 June 2021; published online 25 June 2021)

A comprehensive study on impact of active layer band gap and light illumination on the device performance has been analyzed for the FTO/TiO₂/Cs₂TiX₆/CuSCN/Ag based Perovskite Solar Cell (PSC) using the Solar Cell Capacitance Simulator – 1 Dimension (SCAPS-1D) simulator. The present design strategy of the device for optimizing the short circuit current (J_{sc} , mA/cm²), power conversion efficiency (PCE, %) through the absorbing layer band gap variation, and light illumination spectrum has been studied at the optimal thickness, device temperature, and defect density. The value of the different parameters used in the device simulation has been taken from the previous work. From this study, it was revealed that Cs₂TiBr₆, and Cs₂TiF₆ absorbing layer based PSC device has recorded maximum PCE at the 1.80 eV band gap, whereas, for the Cs₂TiI₆, Cs₂TiCl₆ absorbing layer based PSC device has achieved maximum PCE at the 1.60 eV band gap. On the other side, optimum PCE can be achieved at 400 nm wavelength on the light illumination for the Cs₂TiBr₆, Cs₂TiI₆, and Cs₂TiF₆ absorbing layer based PSC. The Cs₂TiCl₆ absorbing layer based PSC device has recorded maximum PCE at 450 nm wavelength on the different light illumination.

Keywords: Perovskite solar cell, SCAPS-1D, Photovoltaic, Band gap, Illumination.

DOI: [10.21272/jnep.13\(3\).03009](https://doi.org/10.21272/jnep.13(3).03009)

PACS numbers: 42.70.Qs, 84.60.Jt

1. INTRODUCTION

Solar cell is making for the conversion of solar energy into the electrical energy directly, which has undergone through tremendous development from past few years due to its photovoltaic (PV) properties and that creates a huge interest for researcher community to give their attention towards this area. Initially, 1st generation wafer based PV technology was developed but the production cost was relatively higher with lower conversion ability. The production cost became lower after the introduction of thin film based 2nd generation solar cell but still the power conversion efficiency (PCE) remained low. But both the problem including cost and PCE was nullified after the development of thin film based 3rd generation PV technology. Perovskite solar cells (PSCs) has great capability towards photovoltaic applications and is rapidly emerging as 3rd generation solar cell [1, 2]. Due to its highly suitable optoelectronic, physical, mechanical and electrical properties like direct band gap, large charge carrier mobility, higher optical absorption coefficient and higher diffusion length makes it ideal for photovoltaic use [3]. The journey started with Kojima et al. (2009) with halide Perovskite ABM₃ (A: organic CH₃NH₃⁺; B: Pb, X: Br, I) and recorded 3.8 % of power conversion efficiency (PCE, %) [1]. Later, further extensive research on material, deposition process, fabrication methods and device structure has enhanced the PCE up to 20.1 % experimentally and theoretically 31.4 % [4, 5]. Despite of such higher conversion efficiency in laboratory, it has several issues towards the commercialization like environment protection from toxic lead (Pb) component, stability

under environment conditions due to organic component used in ABM₃ structure. To address such issues, researchers are thinking for use of lead-free inorganic material as absorbing material for the photovoltaic applications. Ju et al. (2018) first developed, Cesium Titanium (IV) mixed Halide Perovskite materials which has tunable band gap 1.0-1.8 eV [6]. Chen et al. (2018) achieved 3.28 % PCE, 1.02 V open circuit voltage (V_{oc} , V), 5.69 mA/cm² current density (J_{sc} , mA/cm²) and 56.4 % Fill factor (FF , %) with Cs₂TiBr₆ absorbing material in FTO/TiO₂/Cs₂TiBr₆/P3HT/Au structure [7].

In this study, we have studied the photovoltaic parameters (J_{sc} , PCE) performance with the absorbing layer band gap, light illumination wavelength for the Cs₂TiBr₆, Cs₂TiI₆, Cs₂TiCl₆, and Cs₂TiF₆ based absorbing layer PSC.

2. DEVICE ARCHITECTURE AND SIMULATION

In our proposed FTO/TiO₂/Cs₂TiX₆/CuSCN/Ag based planar solar cell device model, band gap of ETL materials TiO₂ and HTL material CuSCN are taken to be 3.26 eV and 3.4 eV, respectively, the absorbing layer is tunable under 1.6-2.4 eV [8-11]. The working temperature for the simulation was maintained at 27 °C with – 0.8 V to 0.8 V bias voltage in the SCAPS-1D simulator. Here, Fig. 1 shows the schematic view of the proposed structure. All the simulation work was carried out with light illumination of 1.5 AM with the 1000 W/m² light power under Gaussian energy distribution where characteristic energy was set in 0.1 eV. The details of the various properties of the device and the base material taken for the work are shown in Table 1 and Table 2,

* paulsamrat17@gmail.com

The results were presented at the International Conference on Innovative Research in Renewable Energy Technologies (IRRET-2021)

respectively. The symbols i.e., E_g denotes the band gap energy, E_a is the electron affinity, ϵ_r is the relative permittivity, N_A is the acceptor density, N_D is the donor density, N_t is the defect density, N_C is the conduction band effective density of states, N_V is the valence band effective density of states, respectively. Default values of some parameters and settings are as: for electron mobility is $4.4 \text{ cm}^2/\text{Vs}$, the hole mobility is $2.5 \text{ cm}^2/\text{Vs}$, the electron and hole thermal velocity is 10^7 cm/s [12-14].

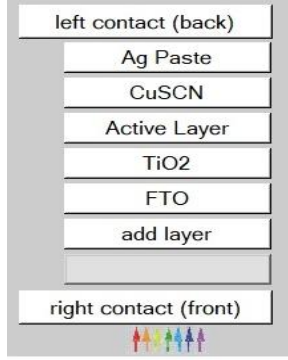


Fig. 1 – Schematic view of the proposed device structure

Table 1 – Base material properties [9, 11, 12]

Properties	CuSCN	TiO ₂	FTO
Thickness (μm)	0.35	0.14	0.1
E_g (eV)	3.40	3.26	3.60
E_a (eV)	1.90	3.70	4.0
ϵ_r	9.0	55.0	9.0
N_D ($1/\text{cm}^3$)	0	4×10^{14}	2.4×10^{18}
N_A ($1/\text{cm}^3$)	1×10^{18}	0	1×10^5
μ_n (cm^2/Vs)	2×10^{-4}	100	100
μ_p (cm^2/Vs)	1×10^{-2}	25	25

Table 2 – Absorbing material properties [6, 7, 13-16]

Properties	Cs ₂ TiBr ₆	Cs ₂ TiI ₆	Cs ₂ TiF ₆	Cs ₂ TiCl ₆
Thickness (μm)	1.5	1.0	1.0	2.5
E_g (eV)	1.78	1.65	1.90	2.23
E_a (eV)	4.47	4.20	3.70	4.0
ϵ_r	10	18	18	19
N_D ($1/\text{cm}^3$)	1×10^{19}	1×10^{19}	1×10^{19}	1×10^{19}
N_A ($1/\text{cm}^3$)	1×10^{19}	1×10^{19}	1×10^{19}	1×10^{19}
μ_n (cm^2/Vs)	4.4	4.4	4.4	4.4
μ_p (cm^2/Vs)	2.5	2.5	2.5	2.5

3. RESULTS AND DISCUSSION

3.1 Effect of Absorbing Layer Band Gap

In this section, various optimal values of the physical parameters, including absorbing layer thickness, device temperature and defect density of halide based absorbing materials (Cs₂TiBr₆, Cs₂TiI₆, Cs₂TiCl₆, and Cs₂TiF₆) have been taken for simulation study under the 300 K. The values of the absorbing layer band gap vary in the range of 1.6-2.4 eV. Here, Fig. 2 shows the changes in J_{SC} and PCE with the band gap variation of the absorbing layer. Theoretically, band gap optimization is important to synthesize an optimized band gap active layer experimentally. From Fig. 2a, it is clearly observed that J_{SC} decreases continuously with the band

gap for Cs₂TiBr₆, Cs₂TiI₆, Cs₂TiCl₆ absorbing layer PSC and for Cs₂TiF₆ absorbing layer PSC; initially J_{SC} increases up to 1.8 eV band gap, then it decreases continuously. Similarly, PCE decreases drastically with the band gap of Cs₂TiI₆, Cs₂TiCl₆ absorbing layer based PSC and for Cs₂TiBr₆, Cs₂TiF₆ PSC the PCE decreases after the 1.8 eV which can be seen in Fig. 2b. The probable reason behind that decrement in the J_{SC} and PCE is much wider band gap of the absorbing layer is leads to less absorption of photons and as a result, low amount of photo-excited carrier is generated in the device. Thus, both the J_{SC} and PCE show decreasing trends with the band gap [17, 18].

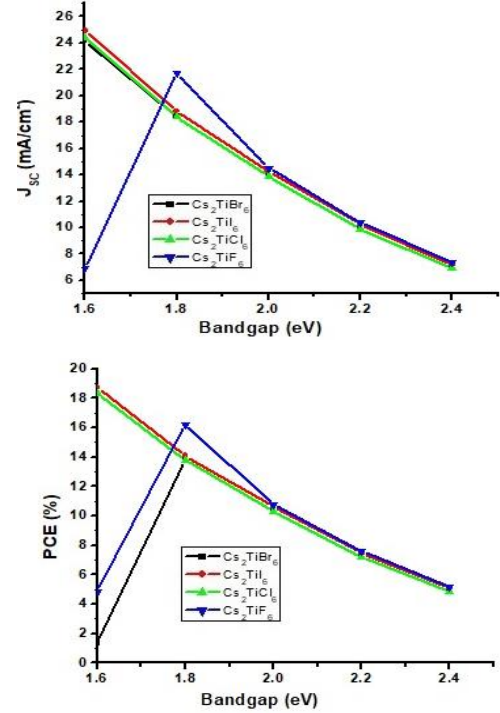


Fig. 2 – Variation in a) J_{SC} and b) PCE with the band gap of the absorbing material

3.2 Effect of Light Illumination Spectrum

In this section, the impact of various light illumination under wavelength of 400 1000 nm on the perovskite solar cell has been studied to analyze the photovoltaic performance of the device. Here, Fig. 3 shows the variation in J_{SC} and PCE with the different wavelength. From this figure it is clear that, Cs₂TiBr₆, Cs₂TiI₆, and Cs₂TiF₆ PSC have almost constant J_{SC} up to 800 nm and after that there is a slight jump in the J_{SC} is observed but for the Cs₂TiCl₆ PSC J_{SC} decreases after 800 nm wavelength. As the J_{SC} is constant up to 800 nm wavelength, the PCE starts to fall from the 400-800 nm wavelength for the Cs₂TiBr₆, Cs₂TiI₆, and Cs₂TiF₆ absorbing layer based PSC and the maximum PCE is recorded as 36 % approximately at 410 nm wavelength. On the other hand, PCE fall drastically from 450 nm wavelength for the Cs₂TiCl₆ absorbing layer based PSC and the highest PCE is recorded as 29 % at 460 nm wavelength. The PCE is depending upon the collection of electron-hole pair generation at the wider wavelength. So, as the illumination wavelength increases, electron-hole pair recombination also increases that leads to decrement in the PCE [19].

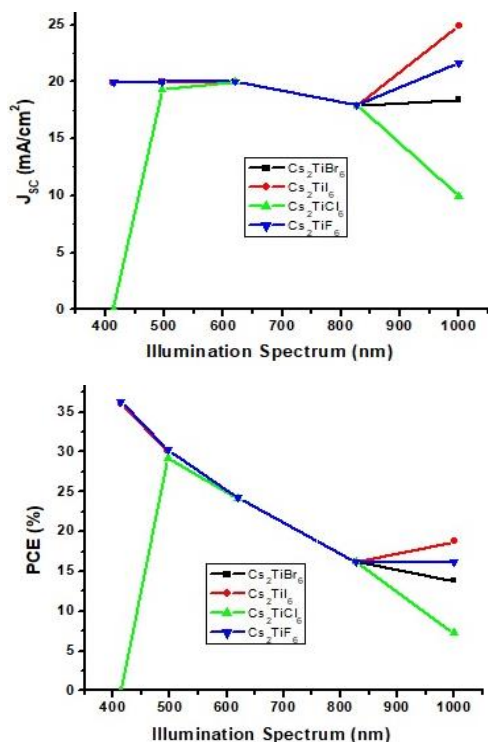


Fig. 3 – Variation in a) J_{sc} and b) PCE with the light illumination spectrum

REFERENCES

1. A. Kojima, K. Teshima, Y. Shirai, T. Miyasaka, *J. Am. Chem. Soc.* **131**, 6050 (2009).
2. F. Giustino, H.J. Snaith, *ACS Energy Lett.* **1**, 1233 (2016).
3. S.D. Stranks, G.E. Eperon, G. Grancini, C. Menelaou, M.J. Alcocer, T. Leijtens, L.M. Herz, A. Petrozza, H.J. Snaith, *Science* **342**, 341 (2013).
4. W.S. Yang, J.H. Noh, N.J. Jeon, Y.C. Kim, S. Ryu, J. Seo, *Science* **348**, 1234 (2015).
5. W.J. Yin, J.H. Yang, J. Kang, Y. Yan, S.H. Wei, *J. Mater. Chem. A* **3**, 8926 (2015).
6. M.G. Ju, M. Chen, Y. Zhou, H.F. Garces, J. Dai, L. Ma, N.P. Padture, X.C. Zeng, *ACS Energy Lett.* **3**, 297 (2018).
7. M. Chen, M.G. Ju, A.D. Carl, Y. Zong, R.L. Grimm, J. Gu, X.C. Zeng, Y. Zhou, N.P. Padture, *Joule* **23**, 558 (2018).
8. W. Ke, G.M. Kanatzidis, *Nat. Commun.* **10**, 965 (2019).
9. N. Chaudhary, R. Chaudhary, J.P. Kesari, A. Patra, S. Chand, *J. Mater. Chem. C* **3**, 11886 (2015).
10. Y. Yang, J. You, *Nature* **544**, 155 (2017).
11. S. Bishnoi, S.K. Pandey, *IET Optoelectron.* **12**, 185 (2018).
12. H. Heriche, Z. Rouabah, N. Bouarissa, *Int. J. Hydrog. Energy* **42**, 9524 (2017).
13. N. Khoshsirar, N.A.M. Yunus, *IEEE Conf. Sustainable Utilization and Development in Engineering and Technology* **1**, (2013).
14. M. Mostefaoui, H. Mazar, S. Khelifi, *Energy Procedia* **74**, 736 (2015).
15. K. Chakraborty, M.G. Choudhury, S. Paul, *Sol. Energy* **194**, 886 (2019).
16. K. Chakraborty, M.G. Choudhury, S. Paul, *IEEE J. Photovol.* **11**, 386 (2021).
17. L. Huang, X. Sun, C. Li, R. Xu, J. Xu, Y. Du, Y. Wu, J. Ni, H. Cai, J. Li, Z. Hu, J. Zhang, *Sol. Energy Mater. Sol. C* **157**, 1038 (2016).
18. K. Tan, P. Lin, G. Wang, Y. Liu, Z. Xu, Y. Lin, *Solid-State Electron.* **126**, 75 (2016).
19. R. Pandey, R. Chaujar, *Superlattice. Microstr.* **100**, 656 (2016).

Вплив ширини забороненої зони активного шару та освітленості на продуктивність пристрою PSC на основі одиночного галогеніду Cs_2TiX_6

K. Chakraborty¹, S. Paul¹, U. Mukherjee², S. Das³

¹ Advanced Materials Research and Energy Application Laboratory, Department of Energy Engineering, North-Eastern Hill University, Shillong-793022 Meghalaya, India

² Department of Life Science, VIT College, Midnapore-721101 West Bengal, India

³ Department of Electronics and Communication Engineering, IMPS College of Engg. and Tech., Malda 732103, West Bengal, India

Комплексне дослідження впливу ширини забороненої зони активного шару та освітленості на продуктивність пристрою було проведено для перовскітного сонячного елемента (PSC) на основі FTO/TiO₂/Cs₂TiX₆/CuSCN/Ag з використанням одновимірному симулятора ємності сонячних елементів

4. CONCLUSIONS

This research article represents the two aspects of design issues of FTO/TiO₂/Cs₂TiX₆/CuSCN/Ag based PSC, band gap of the absorbing layer and light illumination spectrum. The studies show that Cs₂TiBr₆, Cs₂TiF₆ absorbing layers have maximum PCE at the 1.80 eV band gap, and Cs₂TiI₆, Cs₂TiCl₆ absorbing layers have maximum PCE at the 1.60 eV band gap. Similarly, at 400 nm wavelength highest PCE (36 %) can be achieved for Cs₂TiBr₆, Cs₂TiI₆, and Cs₂TiF₆ absorbing layers and at 450 nm wavelength 29 % PCE can be achieved for the Cs₂TiCl₆ absorbing layer based PSC. This simulation-based study can be useful for the selection of desired material at optimal design condition.

ACKNOWLEDGEMENTS

The authors are grateful to the Department of Electronics and Information systems, University of Gent, Belgium, and Prof. Burgelman for providing the SCAPS software for our research. The authors are also thankful to the Science and Engineering Research Board (SERB), Department of Science and Technology (DST) India for their financial support (EMR/2016/002430) to carry out this research work.

(SCAPS-1D). Сучасна стратегія проектування пристрою для оптимізації струму короткого замикання (J_{sc} , mA/cm^2), ефективності перетворення енергії (PCE, %) за рахунок зміни ширини забороненої зони поглинаючого шару та спектру освітленості була досліджена при оптимальних значеннях товщини, температури пристрою і щільності дефектів. Величини різних параметрів, використаних при моделюванні пристрою, було взято з попередньої роботи. Дане дослідження виявило, що для пристрою на основі поглинаючих шарів Cs_2TiBr_6 та Cs_2TiF_6 максимальне значення PCE спостерігається при ширині забороненої зони 1,80 eV, тоді як для пристрою PSC на основі поглинаючих шарів Cs_2TiI_6 та Cs_2TiCl_6 максимальне значення PCE досягнуто при ширині забороненої зони 1,60 eV. З іншого боку, оптимальне значення PCE можна досягти при освітленні з довжиною хвилі 400 нм для PSC на основі поглинаючих шарів Cs_2TiBr_6 , Cs_2TiI_6 та Cs_2TiF_6 . Для пристрою PSC на основі поглинаючого шару Cs_2TiCl_6 зафіксовано максимальне значення PCE при довжині хвилі 450 нм і різному освітленні.

Ключові слова: Перовскітний сонячний елемент, SCAPS-1D, Фотоелектричний, Ширина забороненої зони, Освітленість.